Cell. Mol. Life Sci. 64 (2007) 768 – 780
1420-682X/07/060768-13
DOI 10.1007/s00018-007-6478-3

Cellular and Molecular Life Sciences

Research Article

Circadian changes of ether-a-go-go-related-gene (Erg) potassium channel transcripts in the rat pancreas and β-cell

E. Mühlbauer[a, +, *], I. Bazwinsky[b], S. Wolgast[a], A. Klemenz[b] and E. Peschke[b]

[a] Saxon Academy of Sciences Leipzig, Karl Tauchnitz-Str. 1, 04107 Leipzig (Germany)
[b] Institute of Anatomy and Cell Biology, Martin Luther University Halle-Wittenberg, Grosse Steinstrasse 52, 06097 Halle (Germany)

Received 8 November 2006; received after revision 1 February 2007; accepted 2 February 2007
Online First 23 February 2007

Abstract. Evidence has previously been presented that circadian rhythms play a role in islet hormone secretion. Here, RT-PCR was used to monitor the circadian expression of ether-a-go-go-related gene (Erg) potassium channel isoforms and Erg1 splice variants. Immunohistochemistry was used to identify the pancreatic distribution patterns of ERG1a and ERG1b, as well as ERG2 and ERG3. The influence of ERG on insulin secretion was monitored by perfusion of rat INS-1 β-cells with the blockers E-4031 and rBeKm-1. We identified Erg1a, Erg1b, Erg2 and Erg3 transcripts in islets and INS-1 cells. Immunohistochemistry showed differential expression of ERG isoforms in the islet. Ca^{2+} imaging and electrophysiological recordings of INS-1 cells during ERG blocking by E-4031 indicated functional ERG channels. Serum shock treatment of INS-1 cells elicited a time-dependent expression response for Erg transcripts. These results add to the current understanding of the function of ERG channels in β-cells and the circadian secretion processes of insulin.

Keywords. Insulin secretion, ERG K^+ channel, circadian expression, rat islet function, INS-1 β-cell.

Introduction

The pancreatic islet of Langerhans is the key regulator of blood glucose concentration. Three main peptide hormones, glucagon, insulin and somatostatin, act together in an integrated fashion to ensure glucose homeostasis. Besides external neuronal and gastric impacts, it has recently become evident that the insulin secretion process may also be controlled, in part, from within the islet, creating an underlying pattern of circadian insulin secretion, which becomes evident when the islet is removed from external control during *in vitro* perfusion experiments [1, 2]. We have revealed evidence that a pancreatic peripheral oscillator acts on the islet, creating the circadian secretion pattern observed [3]. The exact mechanism behind the circadian control of insulin secretion still remains elusive. Experiments of Balsalobre et al. [4] using serum shock treatment of rat fibroblasts have proven that the circadian clock is functional even on the level of the single cell. Clock genes may thus act within β-cells to regulate islet genes and functions [5]. Since we did not find direct evidence for a circadian transcriptional regulation of the insulin gene in rat pancreas, a more indirect impact on the insulin release might be transmitted by potassium channels of the β-cell membrane.

[+] Present address: Institute of Anatomy and Cell Biology, Martin Luther University Halle-Wittenberg, Grosse Steinstrasse 52, 06097 Halle (Germany), Fax: +49 345 557 4053, e-mail: eckhard.muehlbauer@medizin.uni-halle.de
[*] Corresponding author.

It is well known that the secretion process of β-cells is triggered by a succession of events initiated by a rise in blood glucose concentration, followed by the metabolic conversion of glucose, and leading to increasing ATP:ADP ratios. Consecutively, K_{ATP} channels are closed, the membrane is depolarized and voltage-dependent calcium channels of the L-type (VDCCs) are opened, increasing the Ca^{2+} concentration of the cell in the vicinity of the VDCCs. The latter event leads to fusion of insulin granula with the cell membrane and subsequent insulin release (reviewed in [6, 7]), a chain of events known as stimulus secretion coupling. In addition to the K_{ATP}, several voltage-gated potassium channels (*e.g.*, Kv1.4, Kv1.5, Kv2.1, Kv2.2, Kv3.1 and Kv3.2) seem to be expressed in the β-cell; these serve as regulators of the membrane potential [8]. Yan et al. [9] listed as many as 17 Kv-channel subtypes in human islets, indicating a very fine-tuned regulation of insulin secretion on the level of membrane potential. According to Itri et al. [10], potassium channels are likely candidates to couple clock-related gene expression to membrane excitability, and thus also to secretion phenomena. Kv3.1b and Kv3.2 in the hypothalamic nucleus suprachiasmaticus (SCN) [10], Kv1.5 and Kv4.2 in heart [11] and the calcium-activated potassium channel Kcnma1 in the SCN [12] reportedly vary in expression levels in a circadian manner. Finally, the ether-a-go-go-related gene channel Erg1 (Kcnh2) was listed as being circadianly expressed in heart by Storch et al. [13]. ERG channels (HERG1 in humans or ERG1 in rats) have attracted interest due to the fact that they are the molecular basis for the long QT-syndrome (LQT2), an inherited cardiac arrhythmia. Thus, evidence exists that circadian control on cellular functions may be exerted *via* changes in potassium channel expression and function.

Rosati et al. [14] were the first to publish results on HERG channel expression in human islets and β-cells using a combination of electrophysiological and molecular techniques to examine the impact of HERG channel action on insulin secretion. Three isoforms (ERG1, ERG2 and ERG3) have been detected in the brain [15], where they supposedly regulate the cell firing rate and hormonal secretion in neuroendocrine cells, and govern the resting membrane potential in other cell types (*e.g.*, lactotroph cells [16]). A transcriptional splice variant of Erg1, *i.e.*, Erg1b, with largely unknown function, seems to be translated into a protein, at least in the central nervous system (CNS) and heart and may be a partner in channel heterodimerization [15, 17]. Interestingly, HERG1a and HERG1b expression are closely linked to the cell cycle and to cell proliferation [18], a process dominated by clock gene activity and which controls cell division. [19]. The importance of pancreatic Erg channel isoforms, and splice variants, however, as well as their distribution within the islet and their function, particularly as putative mediators of clock-driven insulin secretion, are still unknown. The present study is thus aimed at elucidating the expression pattern of Erg channel isoforms and splice variants, both spatially and temporally in the rat pancreas. A possible role of ERG channels in the secretion processes of the rat pancreatic islet was furthermore addressed by employing a well-characterized rat insulinoma β-cell line (INS-1) for functional and circadian analyses.

Materials and methods

Animals and cells

Male Wistar rats (aged 6 weeks) were caged in groups of three animals and subjected to a photo regime of 12/12 h light/dark, with light on at 6:00 a.m. Rats were fed a standard diet *ad libitum*. Five to six animals per sampling were killed in a deep anesthesia at 3-h intervals. All manipulations of the animals proceeded under red light during the dark phase. Animals were treated according to German animal welfare regulations throughout the sampling procedure.

Islets were collected from neonate rats after collagenase treatment as described previously [1] and extracted immediately (approximately at time point T 5). INS-1 cells were cultivated in RPMI 1640, supplemented with 10 % serum until confluence and thereafter collected by trypsination [20].

For serum shock treatment of INS-1 cells, approximately 1×10^5 cells were plated onto 3.5-cm cell culture petri dishes. A modified protocol [21] was used throughout the experiments. Cells were grown for 24 h at 37°C under conditions as previously specified [20]. Thereafter, control dishes received fresh medium with normal 5 % fetal calf serum (FCS), whereas the medium of the treatment group was replaced by RPMI 1640 without serum. After 12 h, the medium was replaced with RPMI 1640 containing high (50 %) horse serum or, in case of controls, with medium including normal serum concentration for 2 h. To stop serum shock treatment, cells (controls as well as high serum-treated cells) were washed twice with phosphate-buffered saline (PBS) and thereafter detached by trypsination and deep frozen until RNA extraction. Times of medium change, temperature und duration of cell handling were carefully kept constant between serum-treated dishes and control dishes to minimize effects other than those of serum treatment.

RNA extraction, DNase 1 digestion and reverse transcription

RNA extraction from pancreata immersed in RNAlater™ (Ambion Inc., TX, USA) and from frozen INS-1 cells or islets proceeded as recently described [3]. DNase 1 digestion (DNA-free™, Ambion Inc.) of total RNA was performed according to the manufacturer's suggestions. For reverse transcription from 1 μg total RNA, a kit from Promega Inc. (WI, USA) and random hexanucleotide primers were used.

Semi-quantitative, real-time RT-PCR

Semi-quantitative, real-time RT-PCR was performed with 40 ng reverse-transcribed cDNA, as recently published [3]. Primers and sequences are listed in Table 1. Each reaction volume of 20 μl contained 10 μl Ready Mix (Promega Inc.), 0.5 μl of each primer (25 pmol/μl), 0.25 μl Eva Green in a 10^3-fold dilution (Biotrend Chemikalien GmbH, Cologne, Germany) and 5 μl H_2O. The runs

Table 1. Primers, sequences and restriction analysis of amplicons.

Gene	Forward primer	Reverse primer	Sequence	Product size, predicted (bp)	Endo-nuclease	Digestion product size, predicted (bp)	PCR product size, determined (bp)	PCR digestion Product size determined (bp)
Erg1a (Kcnh2)	5'-TGGAGAAGGA CATGGTAGGG-3'	5'-GTCAGGTCCA CATCCACCAC-3'	Z96106	205	PvuII	61+144	213	58+153
Erg1b	5'-GGAAGGAGAG CAGGACAGG-3'	5'-GATGGTCCAG CGGTGTATTC-3'	AY669863	164	ApaII	36+128	173	31+128
Erg2 (Kcnh6)	5'-AGATTGGAGT CCCGTGTGTC-3'	5'-TCCCACCAGAA GCGTAGACT-3'	AF016192	165	PvuII	45+120	173	129
Erg3 (Kcnh7)	5'-CGTCTTCCTTT ATCTCCTCC-3'	5'-CTGTAAGATGG CCTGGATGT-3'	AF016191	374	PvuII	181+193	386	196[a]

[a] Not determined separately

were performed on a rotor-cycler from Corbett Research Inc. (Rotor-Gene 2000, Mortlake, NSW, Australia). The PCR reaction conditions were: initial denaturation at 95°C for 120 s followed by 40 cycles with 30 s denaturation at 94°C, 30 s annealing at 59°C (touchdown from 64°C with a 1°C decrease per cycle) and 30 s elongation at 72°C. At the end of each elongation step fluorescence was determined for 15 s at a temperature of 85°C. Each run was followed by determination of a thermal denaturation profile. Relative expression data were determined using the ΔΔCt method and reading the Ct raw data (cycles to threshold level) from the Rotor-Gene 2000 software. Reaction efficiencies for each primer set were calculated from serial dilutions of cDNA. Relative expression values were then corrected for differences in reaction efficiency using the formula and software of Pfaffl et al. [22]. For Erg3, due to the low expression level, a narrative reaction efficiency of 2 was used for calculation. Separation of PCR products proceeded in Tris-acetate-EDTA (pH 8.0)–buffered 3% agarose gels. Control PCRs were performed using PCR reaction mix, including primers without cDNA (non-template control) or with 1 μg total RNA in the reaction mixture (control for DNA carry-over). β-Actin was chosen as a normalizer because there is reportedly no circadian effect on expression [4, 23]. Amplicon identity was examined by gel electrophoresis and restriction enzyme digestion. Results are visualized in Fig. 1 and theoretical band sizes of PCR, as well as those of the digestion products observed, are given in Table 1. Restriction analysis of 10 μl of PCR products with the respective enzyme in a reaction volume of 20 μl was performed for 2 h at 37°C, as recommended by the manufacturer (Promega).

Immunohistochemistry

Male Wistar rats (aged 45 days), kept under the conditions as detailed above, were used for immunocytochemical labeling. The pancreata were immediately fixed by immersion in 4% paraformaldehyde in PBS (pH 7.4) and finally embedded in paraffin. Thin sections (5 μm) were cut on a microtome. Serial sections mounted on glass slides were stained using single- or double-immunofluorescence-labeling methods, basically according to a protocol of Bazwinsky et al. [24].

INS-1 cells were grown directly onto coverslips. Cells were then washed once for 10 min in 1× PBS, and fixed for 10 min at room temperature (4% paraformaldehyde in 1× PBS, pH 7.4) [24]. After two washes in 1× PBS, cells were permeabilized by treatment with 70% ethanol for at least overnight at 4°C. Coverslips could be stored for months at this stage (http://singerlab.aecom.yu.edu/protocols). Following incubation for 20–24 h at 4°C with the primary antibody, goat anti-ERG1a (diluted 1:10, HERG N-20, sc-15966, Santa Cruz Biotechnology Inc. CA, USA), rabbit anti-ERG1b, (diluted 1:40, Neoclone, Madison, WI, USA, [17]) mouse-anti-ERG2 (E78320, diluted 1:100, BD Biosciences, Palo Alto, CA, USA; amino acids 823–937, C-terminal), or rabbit anti-ERG3 (APC-112, diluted 1:50, Alomone; epitope: CPEFL-DLEKSKLKSKE)-treated slides were washed three times in PBS for 15 min. The ERG1b antibody was raised at the ERG1b unique epitope (amino acid 9–23, RTGALQTRAQKGRVR) and was a kind donation of Dr. G. Robertson (University of Madison, WI, USA). These antibodies against ERG1 splice products and their specificities were previously characterized by Western blot experiments [17]. The sections were then incubated for 1 h with 20 μg/ml Cy3-conjugated secondary antibody goat anti-rabbit, or goat anti-mouse, or donkey anti-goat (Dianova GmbH, Hamburg, Germany). The same protocol described above was used for double labeling. The following combinations of primary antibodies were used: (a) mouse anti-glucagon (Sigma, Taufkirchen, Germany, diluted 1:100) and goat anti-ERG1a (diluted 1:10) or rabbit anti-ERG1b (diluted 1:20) or rabbit anti-ERG3 (diluted 1:50) and (b) rabbit anti-glucagon (DAKO GmbH, Hamburg, Germany, diluted 1:100) and mouse anti-ERG2 (diluted 1:100). The secondary antibody mixtures, diluted in 2% BSA in PBS contained: (a) 20 μg/ml goat anti-mouse-DTAF and goat anti-rabbit-Cy3 or donkey anti-mouse-Cy2 and donkey anti-goat-Cy3, respectively, and (b) goat anti-rabbit-Cy2 and goat anti-mouse-Cy3. To test the specificity of anti-ERG1a, anti-ERG2 and anti-ERG3, the antibody solutions were incubated at 4°C overnight with the peptide. Unspecific immunolabeling of the secondary antibody was tested by omission of the primary antibody. The controls confirmed the specificities of the immunolabeling. The immunostaining of ERG1a-, ERG2- and ERG3-specific antibodies was suppressible by their respective control peptides. Pancreatic sections were analyzed under an Axioskop-fluorescence microscope (Zeiss AG, Oberkochen, Germany) equipped with the appropriate filter sets (Zeiss AG) for green and red fluorescent fluorochromes. Images were digitized from representative sections with a CCD camera (Axiocam; Zeiss AG). INS-1 cell images were obtained by laser-scanning confocal microscope Leica TCS SP (Leica, Wetzlar, Germany) equipped with an argon-helium-neon laser and an upright microscope (DMRBE, Leica). Z-series consisted of 512×512 pixel images and were recorded using an × 40 oil-immersion objective and zoom factor 3. Images of a Z-series were combined into a single image using the software program (Scanware, Leica).

Electrophysiological recordings of ERG currents in INS-1 cells

INS-1 cells (0.1×10^6 cells, passages 10–20) were seeded onto glass coverslips (4 mm in diameter), coated with poly-L-lysine (Biochrome, Berlin, Germany) and were used after 3–5 days of incubation. The coverslip was placed into a perfusion chamber

that was mounted on the stage of an inverted microscope (Axiovert 25; Zeiss AG). Perfusion proceeded at a rate of 1 ml/min. Membrane potentials were measured using the perforated patch technique. The extracellular solution contained 125 mM NaCl, 10 mM KCl, 2 mM $CaCl_2$, 2 mM $MgCl_2$, 10 mM HEPES-NaOH and 5.6 mM D-glucose and was adjusted to pH 7.4. Before measurement, the pipette was immersed shortly in the following solution: 140 mM potassium aspartate, 10 mM NaCl, 2 mM $MgCl_2$ and 10 mM HEPES-KOH at pH 7.3. It was back-filled with the same solution containing amphotericin B (150 µg/ml), dissolved in dimethylsulfoxide (stock solution 20 mg/ml). Measurements of E-4031-sensitive currents were carried out in the whole-cell configuration. The bath solution contained 95 mM NaCl, 40 mM KCl, 2 mM $CaCl_2$, 2 mM $MgCl_2$, 10 mM HEPES-NaOH and 5.6 mM D-glucose and was adjusted to pH 7.4. The pipette solution contained 130 mM potassium aspartate, 10 mM NaCl, 2 mM $MgCl_2$, 1.3 mM $CaCl_2$, 10 mM EGTA-KOH, 10 mM HEPES-KOH and 1 mM Mg^{2+}-ATP at pH 7.3 (free Ca^{2+} concentration 10^{-7} M [14]).
All measurements were recorded at room temperature (22°C). Pipette resistance was 3.5–5.5 MΩ. The series resistance and cell capacitance errors were carefully compensated. Measurements were performed using an Axopatch 1b amplifier (Axon Instruments, Sunnyvale, CA, USA) using pclamp 6 software (filtering frequency: 5 kHz).

Perfusion and insulin RIA

Perfusion experiments were performed according to a protocol by Peschke et al. [20], using approximately 4×10^6 INS-1 cells per column. In brief, after packing the cells into glass columns with Sephadex G-10, 1-ml fractions of the eluate with medium 199 were collected in 3-min intervals after a 5-h recovery period. The ERG blockers E-4031 and rBeKm-1 were diluted in PBS and applied in the final concentrations given. Each experimental run was started with a test for cell viability and a standardization of protocol using 20 mM KCl plus either 10 mM arginine or 20 mM glucose for 3-min cell stimulations. This procedure was repeated after application of the toxins and allowed evaluation of possible detrimental toxin effects. All fractions were frozen at –20°C until insulin determination. Insulin levels of the collected fractions (50-µl aliquots) were analyzed by radioimmunoassay (RIA) using a commercial kit (Coat-A-Count; DPC Biermann GmbH, Bad Nauheim, Germany). Series of insulin determinations, *e.g.*, as a response to treatment in perfusion experiments, were calculated from RIA data using software developed by V. Csernus (SUP2, V. Csernus, Department of Anatomy, University Medical School Pecs, Hungary, 2003).

Calcium imaging

Changes in intracellular calcium concentrations were monitored, as recently described in detail [25]. We used a ratiometric method that was originally described by Lipp and Niggli [26], and the two different Ca^{2+} indicators: Calcium Green-1 and Fura Red. During a rise of the Ca^{2+} concentration, Calcium Green-1 shows an increase in fluorescence intensity, while Fura Red fluorescence decreases. Cells grown for 2–4 days on poly-L-lysine-coated glass coverslips were simultaneously loaded with Calcium Green-1 and Fura Red by incubation with 2 µmol/l Calcium Green-1 AM, 4.6 µmol Fura Red AM and 0.02% Pluronic F-127 in the perfusion medium (containing: 140 mM NaCl, 10 mM KCl, 1.2 mM $MgCl_2$, 2.6 mM $CaCl_2$, 10 mM HEPES and 5.6 mM glucose; pH 7.4) for 30–45 min at room temperature in the dark. Ca^{2+}-free perfusion medium contained 1 mM EGTA and replaced the above specified (without $CaCl_2$) during perfusions. Glass coverslips were mounted at the bottom of a closed perfusion chamber (H. Saur GmbH, Reutlingen, Germany). Fluorescence measurements were carried out using an argon ion laser (excitation: 488 nm) and a Leica TCS SP confocal laser scanning microscope attached to a DM IRBE fluorescence microscope (Leica, Heidelberg, Germany) with a ×63 water-immersion objective. Fluorescence emission was detected at 530 and 650 nm, respectively; images of 512×512 pixel were recorded every 5 s. The calculated Calcium Green-1 to Fura Red fluorescence ratio (530:650 nm) indicates the changes in the intracellular concentration of free Ca^{2+}.

Statistical analysis

For calculation of statistical significance of group differences a Mann-Whitney test was performed using Graph Pad Prism (Graph Pad Software Inc., CA, USA), two-way ANOVA was used as indicated. Groups were considered to be significantly different at $p<0.05$.

Results

Analyses of Erg expression

Erg mRNA in tissue and cells. RT-PCR was used to analyze the cellular- and tissue-specific distribution of Erg isoforms using specific primers as specified in Table 1. Transcripts of Erg1a, its splice variant Erg1b, as well as those of isoforms Erg2 and Erg3 were detected as specific RT-PCR products in agarose gels (Fig. 1a; top: bands of Erg1b and Erg2, bottom: bands of Erg3 and Erg1a). With the exception of pancreatic exocrine tissue, in which no PCR products for Erg2 and Erg3 were observed, all transcripts could be visualized in the tissues examined, *i.e.*, in rat brain and pancreas (of animals sacrificed during the day and night time), as well as in islets, pineal cells and INS-1 β-cells. Restriction analysis of islet-derived PCR products verified their specificity, the observed digestion products matching those predicted (Table 1). The two Erg3 digestion products, with a predicted difference of only 12 bp, were not separated on agarose gels but were visible as a ~196-bp double band.

Semi-quantitative, real-time RT-PCR. Comparing relative expression levels of the four Erg transcripts in isolated pancreatic islets of 6-week-old Wistar rats (Fig. 1b), PCR results revealed high levels of Erg1b transcripts. Erg1a and Erg2 transcript levels, on the other hand, were both significantly below those of Erg1b (6.4- and 3.6-fold lower, respectively). The Erg3 transcript level was monitored to be even 8-fold below that of Erg1a, thus being expressed at a level well below that of all other isoforms and Erg1b.
The expression profile of Erg1a indicates changes in transcript abundance during a 24-h period, with a maximum at T11 (Fig. 1c). The expression difference between T11 and the minimum at T14 was 3.4-fold. T0 was defined as the time point of light on. The transcript accumulation of the splice variant Erg1b, in contrast, followed an inverse pattern, with a minimum at T14 and a maximum at T23 (a 3.8-fold difference, Fig. 1d). Erg2 and Erg3 transcripts were measured with maxima at T11 and T14, respectively. Expression minima were recorded at T14 for Erg2 and at T2 for Erg3 transcripts, differences between time points of the maximum and

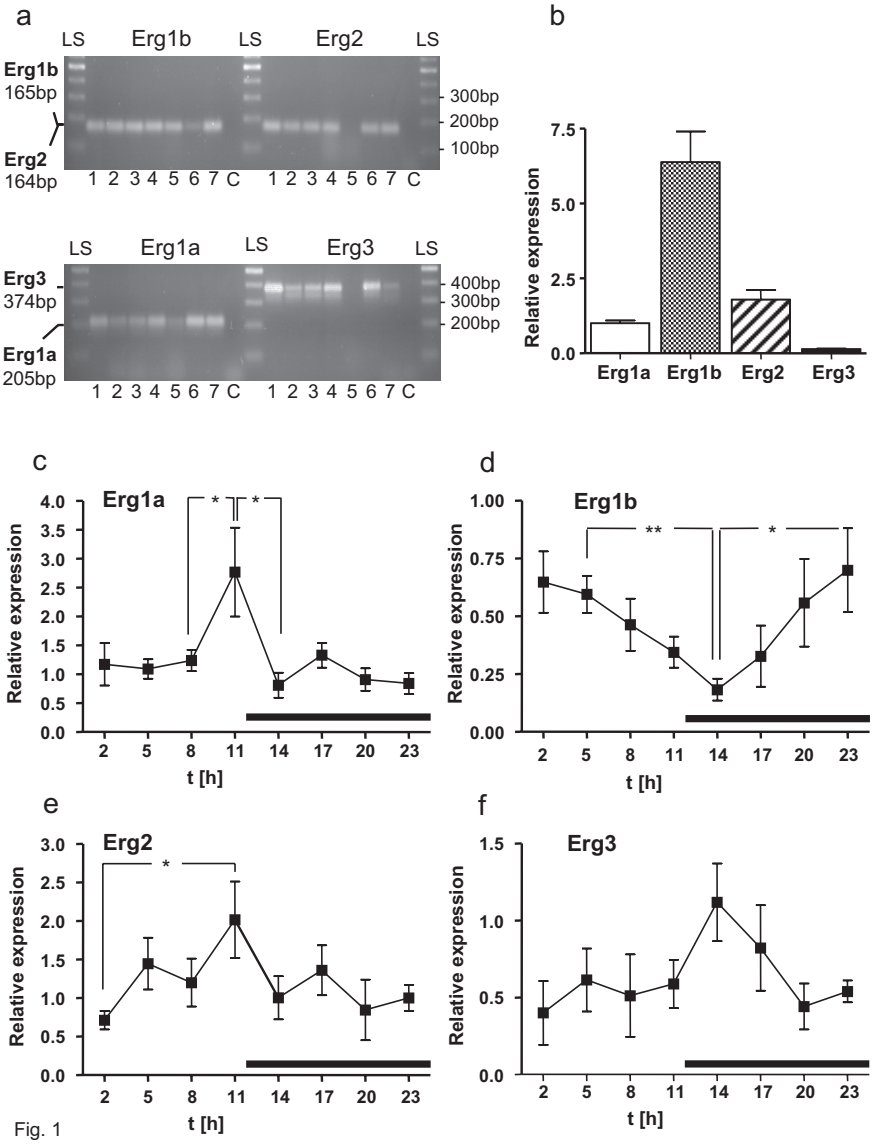

Fig. 1

Figure 1. RT-PCR analysis of Erg isoforms and splice variants. (a) Expression patterns of Erg1 to Erg3 potassium channel genes and splice variants in pancreatic and control rat tissue, indicated by PCR-dependent transcript detection. RT-PCR products of Erg1b and Erg2 (top) or Erg3 and Erg1a (bottom) are shown after gel-electrophoretic separation on 3% agarose gels. The results provide evidence that the transcripts of all Erg channel isoforms including those of the two Erg1 splice variants are present in rat pancreatic islets and INS-1 insulinoma β-cells. Band: 1, brain; 2, pancreas (day); 3, pancreas (night); 4, pancreatic islets; 5, exocrine pancreas; 6, INS-1 cells; 7, pineal; C, non-template (H_2O) control. Molecular sizes of the respective PCR products are indicated relative to a molecular size standard (LS). (b) Relative expression levels of Erg isoforms and Erg1 splice variants in pancreatic islets, indicating Erg1b as the predominant transcript. Expression differences between all Erg isoforms in islets were statistically significant, with the exception of expression levels between Erg1a and Erg3 ($p<0.05$, $n=4$, Mann-Whitney test). Circadian expression patterns of Erg potassium channel genes in the rat pancreas (c–f). Quantitative real-time RT-PCR results of four to six animals per time point. Data are expressed as means (± SEM). T0 was defined as light on. (c) Circadian changes of Erg1a mRNA-derived PCR products. (d) Circadian changes of the Erg1 splice variant Erg1b, demonstrating transcript levels with a largely inverse expression pattern relative to Erg1a. (e) Expression pattern of Erg2 mRNA-derived PCR products. (f) PCR products of the Erg3 transcript. A thick horizontal bar indicates duration of the time period with the light off. Asterisks indicate statistically significant differences between time points at $p<0.05$ (Mann-Whitney test).

minimum expression were calculated to be 10.6-fold for Erg2, but only 2.8-fold for Erg3 (Fig. 1e, f).

Characterization of Erg channel isoform expression in INS-1 cells and effects of serum shock treatment. To analyze the range and quantity of Erg channel isoforms and splice variants in INS-1 β-cells, we performed quantitative real-time RT-PCR experiments. As presented in Fig. 2a, the predominant transcript is attributed to Erg1a in the rat β-cell line. A very low level was measured for the splice variant Erg1b (0.01% of Erg1a mRNA). Erg2 and Erg3 transcripts

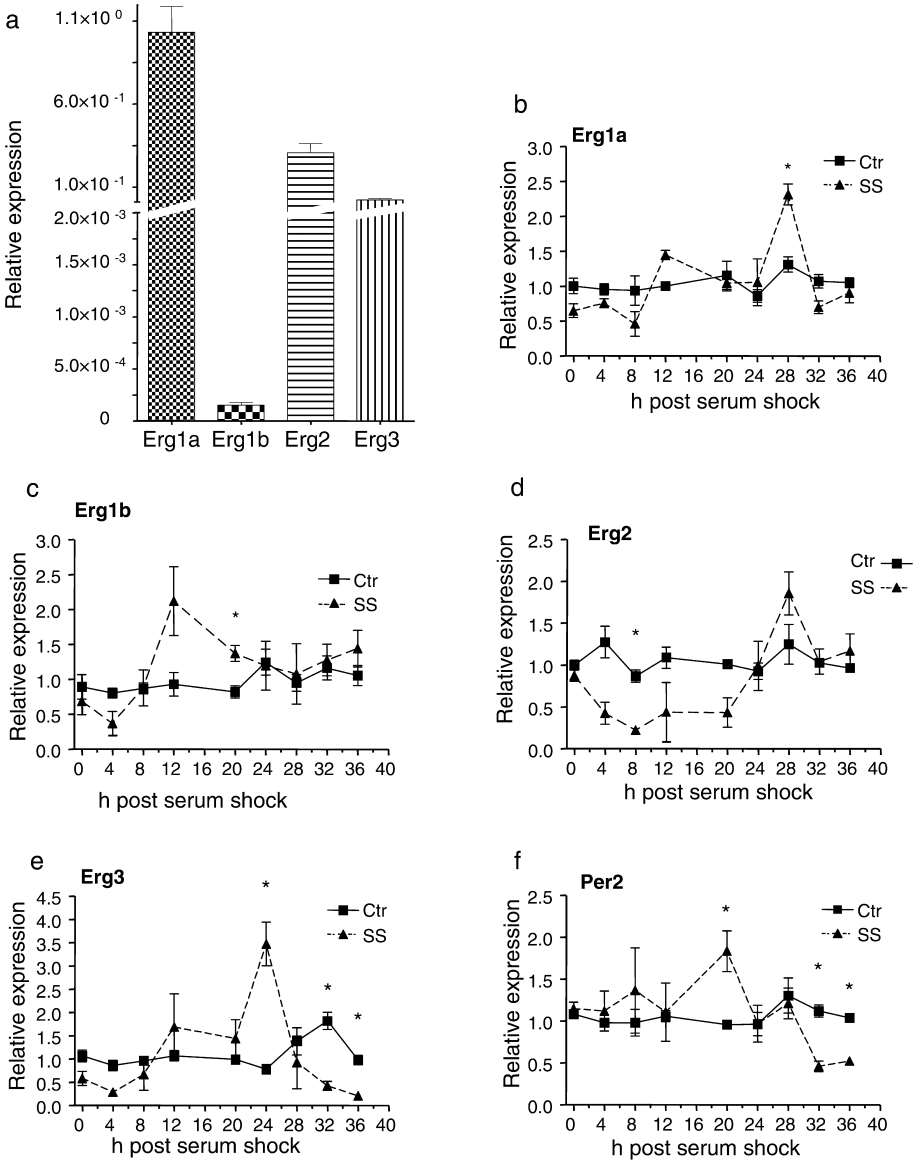

Figure 2. RT-PCR analyses of Erg transcripts in INS-1 insulinoma β-cells. Relative expression levels of the Erg potassium channel isoforms and splice variants in INS-1 insulinoma cells indicating Erg1a as the major Erg1 splice variant in INS-1 cells with a low level of Erg1b expression (a). Erg2 and Erg3 transcript levels were well below that of Erg1a. Quantitative differences between the four isoforms or splice variants were statistically significant ($p<0.05$ for $n=4$ cell batches, Mann-Whitney-test). Serum shock treatment-elicited Erg channel expression changes in treated cell batches compared to control cells. Increased expression 24–28 h after serum treatment for Erg1a (b), Erg2 (d) and Erg3 (e) was measured. Erg1b was monitored to accumulate earlier, approximately 12–20 h after serum shock (c). The clock gene Per2 indicated an expression maximum 20 h after serum shock (f). Significant differences of expression at distinct time points between control and serum shock samples are indicated by asterisk.

were determined to be 28% and 2.1% of the Erg1a expression level, respectively.

Induction of circadian rhythms by serum shock is a well-established technique to test the induction of gene expression to susceptible genes [4]. The same technique was used by Allaman-Pillet [5] for the expression study of the clock gene and clock gene - driven genes in a mouse β-cell line. Our own protocol, employing the rat INS-1 cell line, indicates that the three Erg channel isoforms Erg1a, Erg2 and Erg3 respond to serum shock treatment of the cells by up-regulating their respective transcripts 28 or 24 h after serum shock (Fig. 2b, d, e). The splice variant Erg1b displayed a different pattern from that of Erg1a, the mRNA was found to accumulate earlier at 12–20 h post serum shock (Fig. 2c). A significant effect of time was calculated for serum shock-treated cells for Erg1a, Erg2 and Erg3, but not for Erg1b transcript levels (ANOVA, p at least <0.01). A significant effect of serum shock was also monitored for the clock gene Per2 ($p<0.05$) (Fig. 2f), indicating impact of a cell internal circadian clock.

Immunohistochemistry of rat pancreas and INS-1 cells. Analysis of ERG protein expression in INS-1 cells by immunostaining with specific antibodies for ERG1a, ERG1b, ERG2 and ERG3 indicates that all isoforms and splice variants are expressed in this rat β-cell line (Fig. 3d, h, l, p), which corresponds to the pattern of transcripts detected in INS-1 cells (Fig. 2a). Examination of pancreatic tissue from 6-week-old rats with specific antibodies for ERG1a, ERG1b, ERG2 and ERG3 revealed that the two ERG1 splice variants and all three channel isoforms were expressed in the

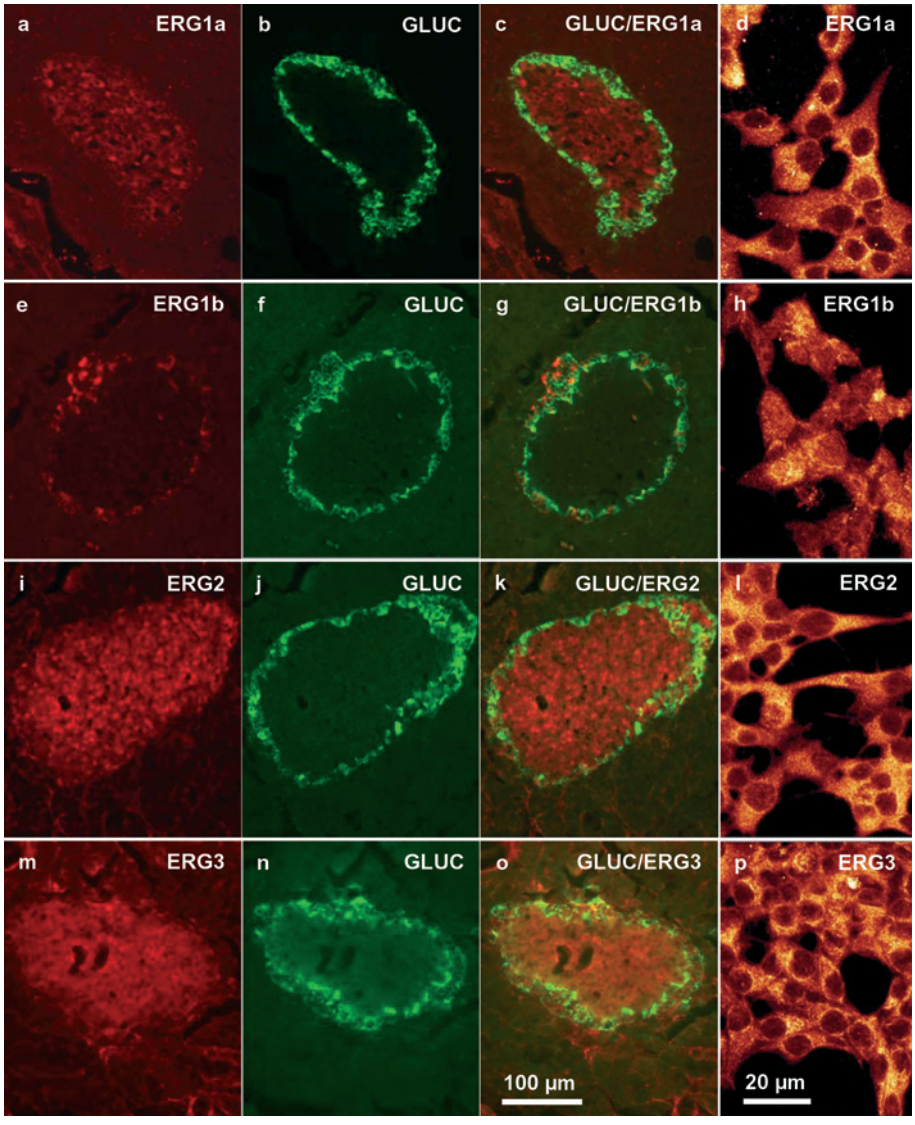

Figure 3. Visualization of the ERG1a, ERG1b, ERG2 and ERG3 distribution patterns in rat pancreatic islets by immunohistochemistry. (a) ERG1a immunolabeling, concentrated on islets and distribution within the islet. (b) α-cell distribution within the islet as visualized by glucagon immunoreactivity. (c) Double immunolabeling with anti-glucagon- and anti-ERG1-specific antibodies supporting primarily β-cell expression of ERG1a. (d) ERG1a immunolabeling of INS-1 β-cells. (e) ERG1b immunolabeling of islets. (f) Glucagon labeling of α-cells. (g) Double labeling with glucagon- and ERG1b-specific antibodies, indicating primarily α-cell expression of ERG1b. (h) ERG1b-labeling of INS-1 cells. (i) ERG2 immunofluorescence within the pancreatic islets, with strong labeling of β-cells. (j) Glucagon-positive cells of the same islet. (k) Double labeling with anti-glucagon and anti-ERG2; the latter is expressed in both α- and β-cell types. (l) Positive immunoreaction of INS-1 β-cells with anti-ERG2. (m) Pancreatic ERG3 immunolabeling is of low intensity and dispersed throughout the islet. (n) Glucagon-positive cells of the same islet. (o) Co-expression of peripheral glucagon and ERG3, which is distributed throughout the islet. (p) Immunopositive labeling of INS-1 β-cells with anti-ERG3.

islet of Langerhans (Fig. 3a–c, e–g, i–k, m–o). However, employing specific antibodies for ERG1a and ERG1b, a striking difference in cell-type expression was noted. α-cells and δ-cells, which are located on the periphery of rat islets or dispersed throughout the islet (δ-cells), seemed to be largely devoid of ERG1a-specific immunofluorescence (Fig. 3a) as double staining with a glucagon-specific antibody suggests (Fig. 3b). ERG1a was found to be concentrated on β-cells, which are exclusively centrally located in rat islets (Fig. 3c). In contrast, the ERG1b immunofluorescence was largely confined to the peripheral ring of α-cells (Fig. 3e–g) with no or minor central labeling, indicating low level expression in β-cells (Fig. 3 g). No, or little, ERG immunofluorescence was detected in the exocrine tissue surrounding the islets (Fig. 3a, e, i, m). ERG2- and ERG3-immunopositive cells, in contrast to the ERG1 variants, could be detected throughout the islet (Fig. 3i–k, m–o). This result implies that ERG isoforms 2 and 3 are expressed in islet cells and spatially overlap in α- as well as β-cell areas. In contrast, expression of the two splice variants of ERG1 seems to be largely linked to either the β-cell (ERG1a) or the α-cell (ERG1b) and their specific functions.

Functional analyses of ERG in INS-1 cells

Electrophysiological effects of the Erg channel blocker E-4031 on INS-1 cells. The influence of the blocker E-4031on the membrane current and the membrane potential was investigated on the INS-1 insulinoma cell, which is a widely used model for β-cell functions [27]. The experiment was aimed at elucidating pharmacologically relevant effects of E-4031 due to ERG channel blocking as an indication of ERG channel expression and function in INS-1 cells. To identify E-

4031-sensitive currents, the voltage clamp method was used with protocols shown in Figure 4a and b (top panels), with the holding potentials 0 and –60 mV, respectively. These protocols were chosen since it is known that ERG channel isoforms are differentially inactivated below a potential of –44 mV (ERG3) through –20 mV (ERG1) to –3.5 mV (ERG2) [16, 28], and are activated using a holding potential of 0 mV. E-4031-sensitive currents were calculated as the difference of membrane current recordings without and with the blocker and are presented in Figure 4a and b (bottom), original current recordings are not shown. Using the voltage protocol (illustrated in Fig. 4a, top), E-4031 sensitive currents occurred (Fig. 4a, bottom). Compared to the control, the blocker led to a reduction of the membrane current at 0 mV holding potential by 12.2±2.4 % (mean ± SEM, n=6). Using the voltage protocol of Figure 4b (top), no E-4031-sensitive currents were measured (Fig. 4b, bottom) because ERG channels are known to be inactive below clamp voltages of about –50 mV [16, 27]. Current clamp membrane potentials, measured in the perforated patch configuration, are illustrated as a time-course recording from an INS-1 cell in Figure 4c. The tolbutamide-induced depolarization accompanied by spiking indicates expression of the β-cell-specific K_{ATP} (Kir6.2/SUR1) channel. Application of 40 mM KCl resulted in strong membrane depolarization. Addition of E-4031 elicited a small, but clearly detectable, cell membrane depolarization (4.4±0.8 mV, mean ± SEM, n=9) as an indication of blocking the ERG channel in INS-1 cells. The influence of the blocker E-4031 on the membrane currents as well as the membrane potential suggest expression of functional ERG channels in the INS-1 insulinoma cell.

Perfusion experiments with INS-1 cells using pharmacological ERG blockers. To test the hypotheses of expression of functional ERG channels in INS-1 cells and their influence on insulin secretion, perfusion experiments using the known methanesulfonanilide ERG channel blocker E-4031 [28] and the recently described scorpion peptide toxin rBeKm-1 [29] were performed. Insulin concentrations of the eluted fractions indicated that E-4031 elevated insulin secretion at concentrations as low as 0.1 μM (Fig. 5a). Secretion augmentation could be induced by consecutive applications of 10 and 1 μM of the blocker within the same experiment. Glucose (20 mM) and KCl (20 mM) stimulations at the end of the experiment elicited a similar response to that at the beginning of the experiment and thus indicated integrity of the cells and of the secretion machinery. As illustrated in Figure 5b, the peptide blocker of ERG1, rBeKm-1 [29], also leads to enhanced insulin secretion from INS-1 cells; thus, both chemically distinct blockers point to a functional role of ERG1 in the insulin-releasing process. The arginine-assisted perfusion experiment (Fig. 5c) also indicated that addition of E-4031 leads to an additional insulin surge, with as little as 0.1 μM E-4031. Mean values from three experiments for the insulin secreted during E-4031 blocking of INS-1 cells are presented in Figure 5c, indicating a dose–response relation for this sulfonylanilide in a range from 0.1 to 10 μM.

Effects of E-4031 on calcium concentrations of INS-1 cells. The influence of ERG channel activity on changes of the intracellular calcium-concentration was assessed to test the idea of a modulation of insulin secretion by changes in β-cell calcium concentration. The ERG-specific blocker E-4031 was used on INS-1 cells for that purpose. Calcium imaging employing the dual Ca^{2+}-indicator technique of Lipp and Niggli [26] was performed. An intracellular calcium increase is measured as a change in the Calcium Green-1 to Fura Red ratio (visualized in Fig. 6a). Using an extracellular medium with 5.6 mM glucose and 10 mM KCl, perfusion of the cells with 1 μM E-4031 for 180 s elicited a transient increase in intracellular Ca^{2+} (Fig. 6b), presenting a representative recording from one cell. Similar signals were elicited by 43 % of the cells (from 227) from 11 perfusion experiments. The increase in the fluorescence ratio (530:650 nm) above base level amounted, on average, to 16.3±1.4 % (n=97). This change in intracellular Ca^{2+} concentration, however, was not detectible in control experiments using a Ca^{2+}-free perfusion buffer. Figure 6c shows a representative example from 1 cell (out of 153) of 9 stimulation experiments. Thus, the observed increase in calcium concentration during an E-4031 block of ERG channels presumably resulted from extracellular sources exclusively. These data indicate the existence of functional ERG channels in the INS-1 cellular membrane. We suspect that their action is, at least in part, responsible for maintaining membrane potential and regulation of cell excitability [16].

Discussion

It is not yet known how insulin secretion from isolated islets, when transferred into a column during *in vitro* experiments, as performed by Peschke and Peschke [1] and Picinato et al. [2], is regulated in a circadian manner. It is conceivable that components of a pancreatic circadian clock (*e.g.*, PER/CRY and BMAL1/CLOCK dimers [3]) exert their influence on insulin in a direct way *via* E-box elements of the insulin

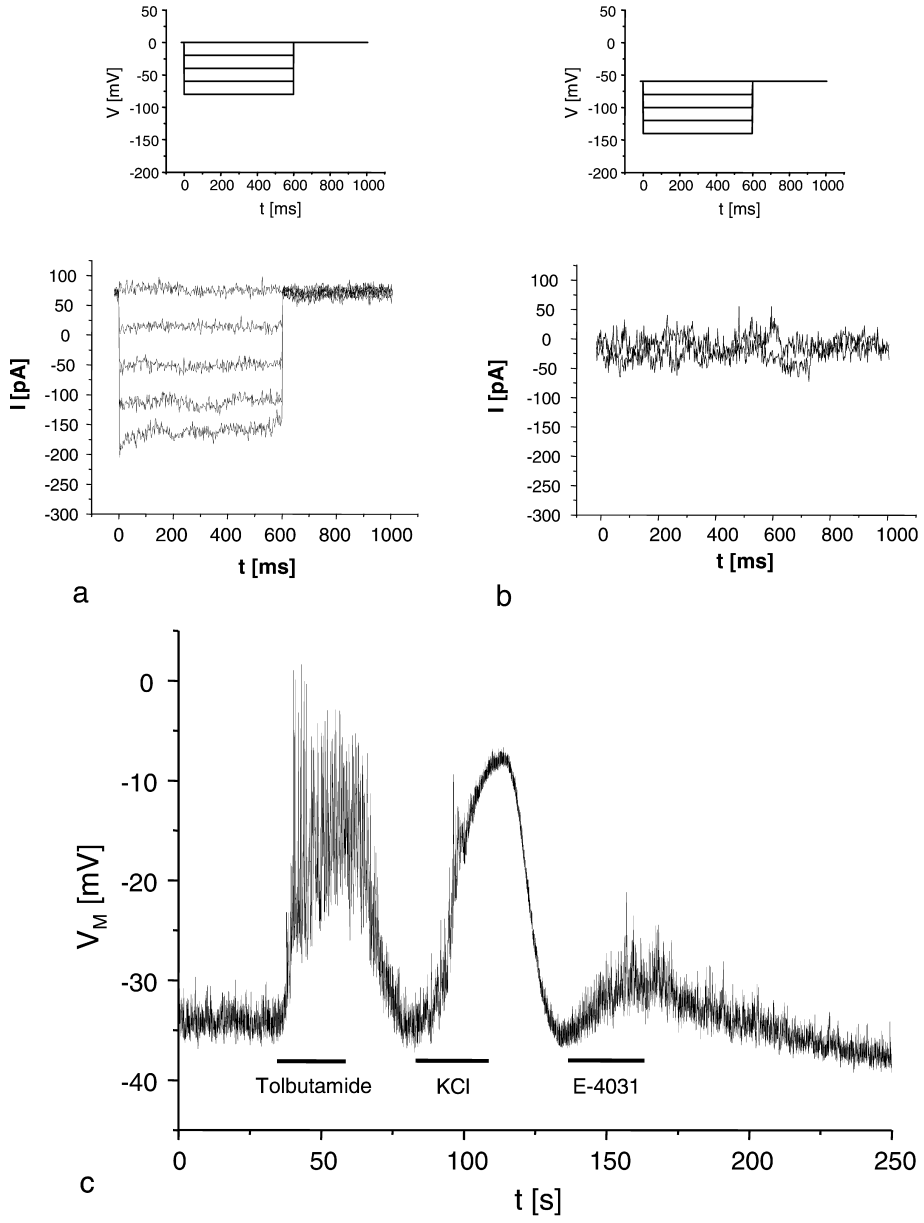

Figure 4. Electrophysiological and pharmacological determination of ERG channel activity in INS-1 insulinoma β-cells. The middle panel (a, b) present E-4031-sensitive currents that are defined as the result of subtracting currents, measured without and during perfusion with E-4031 (1 μM). The voltage protocols used are presented above. (a) Bottom: E-4031 sensitive currents in INS-1 cells at a holding potential of 0 mV. (b) bottom: If the cells were clamped to voltages of –60 mV and below, no E-4031-sensitive currents were observed. (c) Original recording of the membrane potential of an INS-1 cell sequentially stimulated by: tolbutamide (10 μM), KCl (40 mM) and the ERG channel blocker E-4031 (1 μM). The K_{ATP}-channel blocker tolbutamide led to a depolarization and elicitation of action potentials, which were also visible after stimulation with KCl. The blocking of ERG channels by E-4031 induced a small membrane depolarization. V_M, membrane potential; I, E-4031-sensitive current.

promoter [30]. In addition, circadian effects could be exerted by clock output genes like Dbp, RevErbα, or RORβ (their products binding to promoter D-box elements or RevErbα/ROR binding elements (RREs), respectively [31]). We did not, however, find a clear circadian pattern in the insulin transcript accumulation in rat pancreas (data not shown). The influence of circadian timing on the secretion process may thus be indirect, either by acting on vesicle transport and fusion [12] or on other critical components of the secretion process. In an attempt to screen for elements of the insulin secretion machinery that might be regulated in a circadian fashion, the potassium channel genes Erg1 (with splice variants a and b), Erg2 and Erg3 were found to vary in their transcriptional activity during a circadian period. This result substantiates data from a recent study by Storch et al. [13]. These authors used an array technique for detecting time-dependent transcript fluctuations in mouse heart or liver (>12 000 genes), and listed Erg1 to be among the 8–10% of circadian clock-driven genes detected. Furthermore, we determined that the Erg1a transcript changes in rat pancreas were in-phase with Per1-mRNA changes. Surprisingly, the Erg1 splice variant Erg1b was expressed anti-phase to Erg1a (thus, in-phase with the Bmal1 transcript [3]). Our hypothesis of a circadian impact on Erg gene expression is substantiated by the results from serum shock experiments on INS-1 cells. These data speak in favor of a circadian transcriptional regulation of the three Erg genes leading to time-

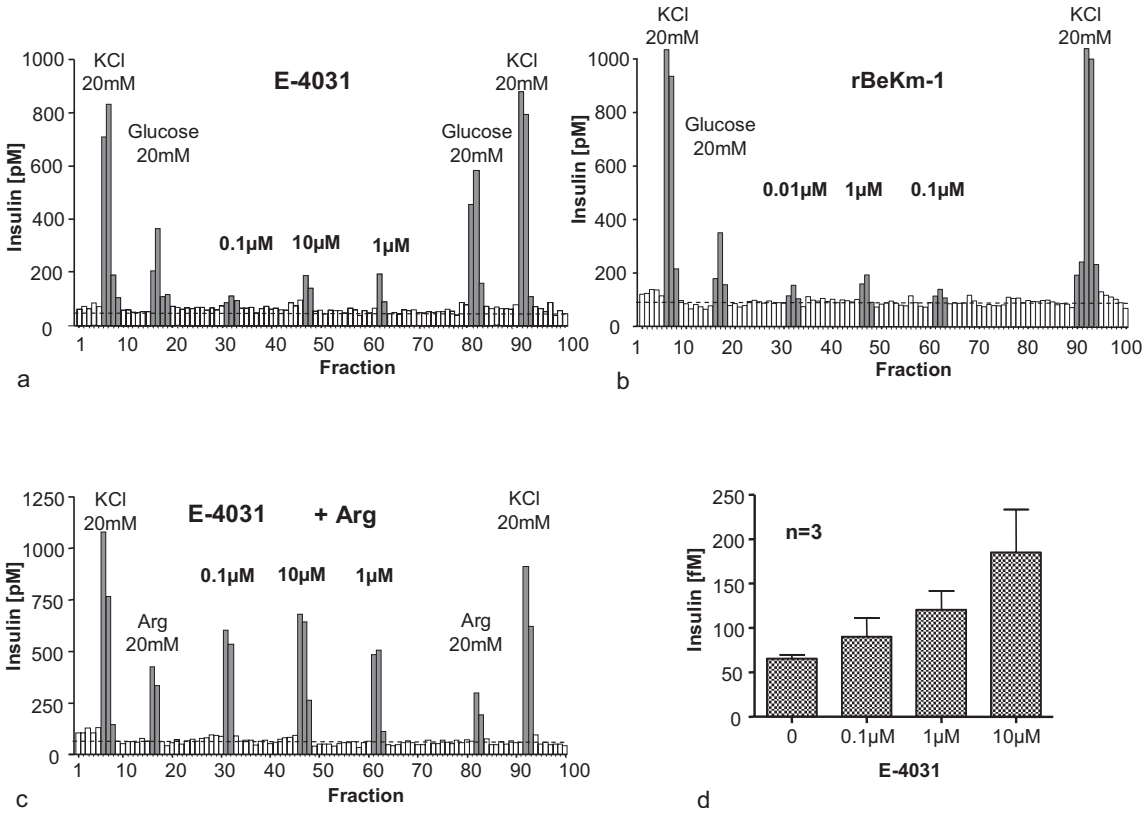

Figure 5. Perfusion experiments with rat INS-1 insulinoma β-cells. (a) The insulin-liberating effect of the methanesulfonalide ERG channel blocker E-4031 alone is shown. Stimulation of the cells by 20 mM KCl and 20 mM glucose before and after treatment with the toxin served as internal controls for cell viability. (b) The insulin-liberating effect of the scorpion peptide-toxin rBeKm-1 is shown. (c) The effect of E-4031 on insulin secretion, facilitated with 10 mM arginine during periods of blocker application, is illustrated. Insulin peaks, following cell stimulation (after a 3-min time lag or one fraction collected), are shaded in gray. A stimulatory effect of ERG channel blocking by E-4031 on insulin secretion is dose dependent (d). Average values of three experiments are represented in the concentration range indicated (area under the curve). Individual bars in (a–c) represent the insulin concentration of the collected medium flow of 3 min (1 ml).

dependent peaks of transcript accumulation with different phases for Erg1a and Erg1b. These results are in accord with Allaman-Pillet et al. [5], who showed β-cell internal rhythms to be elicited in the β-cell line β-TC-3. In contrast to results of Allaman-Pillet et al. [5], who found evidence for circadian expression of the insulin gene (Ins) after serum shock, we were not able to directly monitor a clear circadian expression rhythm for Ins in the rat pancreas, although circadian oscillations of other genes were clearly monitored [3]. However, low-level amplitudes may have escaped our detection, and there may thus still be a direct circadian influence on insulin gene transcription *in vivo,* as implied by the aforementioned authors. Since the INS-1 cell line is known to proliferate very slowly (doubling time ~100 h [32]) the observed pattern of transcript accumulation cannot be explained by the mitotic activity of the cells. The results thus indicate that the pancreatic β-cell (INS-1) seems to carry its own clock for creating circadian rhythms that impinges on potassium channels like ERG.

Guasti et al. [15] reported that the Erg1b transcript is translated into a functional protein in the brain and possibly co-assembles with ERG1a in the CNS. According to Lees-Miller et al. [33], ERG1b is an essential contribution to the inwardly rectifying $I_{(Kr)}$ in mouse heart. Knockout led to bradycardia in their mouse model. Both splice variants expressed in a coordinated fashion in pancreas might, thus, also be of importance in secretion processes. Surprisingly, the ERG1b-specific antibody used by Jones et al. [17] detected specific immunostaining in the periphery of the islet only, largely matching the area of glucagon immunoreactivity, although low-level ERG1b expression was monitored in INS-1 cells and as a transcript in islets. A spatial, and therefore likely also functional, dissection of the two Erg1 splice variants has not been reported from other cell types or tissues. Assuming that functional ERG1b channel proteins co-exist with ERG2 and ERG3 in pancreatic α-cells would suggest a change in ERG channel composition involving both isoforms and the splice variant with anti-phase expression over a 24-h period. Our experiments by RT-PCR indicated that all four Erg transcripts can be

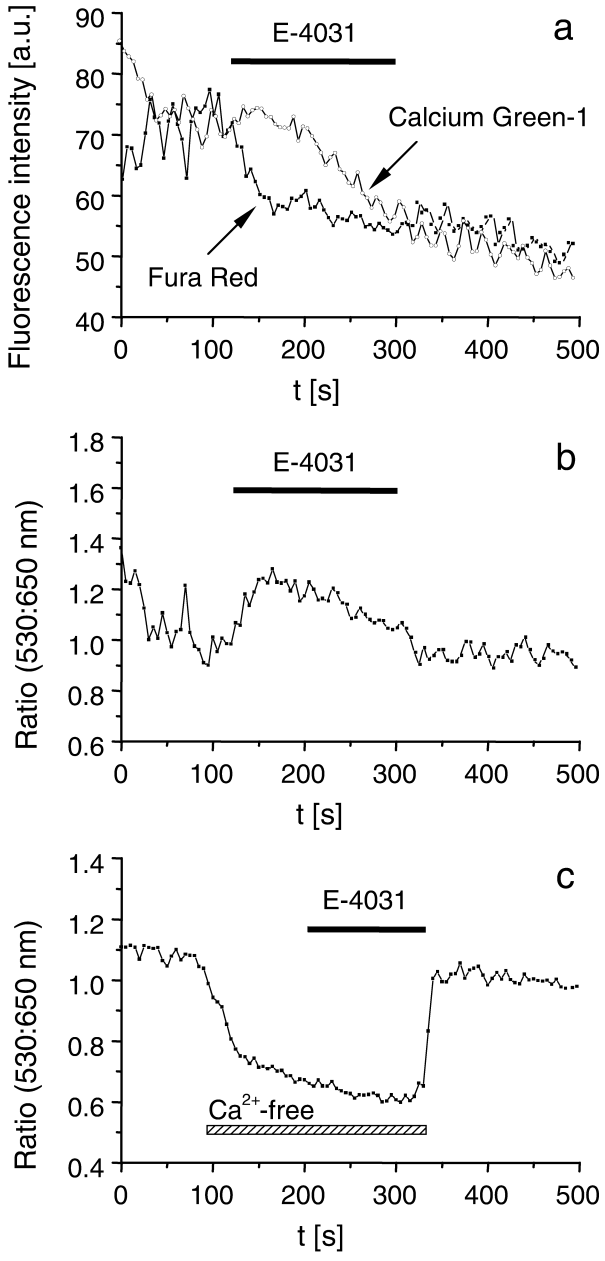

Figure 6. Calcium imaging of INS-1 insulinoma β-cells emphasizing the calcium mobilizing effect due to ERG channel blocking by 1 μM E-4031. (a) Fluorescence emission (in arbitrary units, a.u.) of a representative single INS-1 cell. ERG channels were blocked with 1 μM E-4031 as indicated by the black horizontal bar. The blocking leads to changes in the fluorescence emission. The emission of Calcium Green-1 (530 nm) increases, while the emission of Fura Red (650 nm) decreases. This indicates an increase in intracellular Ca^{2+} concentration. Both traces continuously decrease in fluorescence intensity as a result of bleaching. (b) Fluorescence ratio 530:650 nm obtained after division of fluorescence traces presented in Fig. 6a. A recognizable change in Ca^{2+} concentration is detectable on blocking ERG channels with 1 μM E-4031. (c) Representative plot of one single INS-1 cell as presented in Fig. 6b, but without Ca^{2+} in the extracellular solution. As indicated by the horizontal hatched bar, cells were rinsed with Ca^{2+}-free medium. Addition of 1 μM E-4031 (marked by horizontal black bar) did not result in a change of Ca^{2+} concentration. There is no obvious mobilization of Ca^{2+} from intracellular sources after blocking of ERG channels with E-4031.

detected in islet and INS-1 β-cells, thus pointing to the islet and β-cell-specific functions of these genes and splice variants, although the Erg1b transcript level was low in INS-1 cells. The notion of a primarily islet-specific function is supported by the fact that no PCR product for Erg2 and Erg3 was detected in exocrine tissue. As visualized by co-staining with anti-glucagon, the ERG1a immunoreactivity was largely detectable in (centrally located) β-cells, and not, or to a lesser extent, in peripheral α- and δ-cells, thus also confirming a specific function for this channel in β-cells. Our results support a possible assembly of homotetrameric channels of either splice variant within the particular islet cell type or association with other isoforms (ERG2 and ERG3), a possibility suggested by Wimmers et al. [34]. We found that, in contrast to ERG1a, and ERG1b, ERG2 and ERG3 immunoreactivity encompassed the entire islet, including the periphery. The isoform Erg3 seemed to be expressed at a low level only, as indicated by islet transcript quantification; Erg1b demonstrated the highest transcript levels observed. The low abundance of Erg3 transcripts in islets was matched by a low level of islet immunostaining. Analyzing basal transcript levels of the β-cell line INS-1, we found, in accord with immunolabeling of the islet, only low-level Erg1b expression in the β-cell.

All three known isoform channel transcripts and proteins (ERG1 with splice variants a and b, ERG2 and ERG3) were detected in rat islets in this study, in contrast to the general notion of a primarily neuronal expression of the latter two [15, 35]. Whether heteromultimeric channel assembly of ERG isoforms [34] leads to functional channels in islets, and particularly in β-cells, remains to be examined in more detail. The spatial overlapping of isoform immunodetection in the centrally located β-cells makes the occurrence of heteromultimeric channels at least conceivable. The importance of ERG for α- or δ-cell function is still unknown, although α-cell expression of ERG1b, ERG2 and ERG3 seems to be detectable in our experiments.

Our perfusion experiments point to an ERG channel function within the context of islet physiology. Blocking ERG channel activity with E-4031 or rBeKm-1 resulted in a clear and reproducible increase in basal insulin secretion from INS-1 β-cells. For E-4031, a dose response was linear in the range between 0.1 and 10 μM. No clear dose-response relationship was observed for rBeKm-1, although the doses chosen were within the range of concentrations used by others (albeit on neuronal cells [29]). In accordance with electrophysiological data from Rosati et al. [14], arginine enhanced the ERG channel blockers E-4031 and rBeKm-1 under low glucose (3 mM) con-

ditions. The same authors also suggested ERG-blocker-induced hyperexcitability to be the driving force behind insulin secretion from β-cells. Our observations that E-4031-sensitive potassium currents are elicited at a voltage clamp of 0 mV point to the existence of functional ERG channels in the INS-1 cell membrane. Similarly, Rosati et al. [14] found evidence of functional HERG channels (human ERG1 homolog) in human primary β-cells, using the methanesulfonanilide Way 123,398 as a blocker. The perforated patch membrane potential recordings, which showed E-4031-induced depolarization, further substantiate expression of functional ERG potassium channels in the INS-1 β-cell membrane. Compared to KCl-induced effects, ERG-dependent depolarization seems to be rather minimal, but may be larger in a native cell environment at other times in a circadian period.

Little is known about calcium mobilization due to ERG channel blocking in excitable cells. Overholt et al. [36] reported depolarization-induced calcium influx as a response to a dofetilide block of HERG channels in rabbit carotid glomus cells. In accordance with their findings [36], our data from calcium-imaging experiments also indicate a mechanism of cell membrane depolarization. This leads to calcium intrusion from the extracellular milieu during the action of the ERG blocker E-4031 in INS-1 insulinoma cells. The mobilization from intracellular sources seems to be a negligible effect. This observation led us to conclude that the enhanced insulin secretion is caused by a Ca^{2+}-dependent mechanism; it also suggests that ERG channels have a functional role in INS-1 cells. Here, they may be part of a group of inwardly rectifying K^+ channels, which control the resting membrane potential. Due to their supposedly circadian fluctuation, ERG channels may be specialized members of the inwardly rectifying K^+ channels, which transmit changes in membrane repolarization during a circadian period with impact on firing frequency and perhaps burst rate. As a consequence, the pattern of basal insulin secretion would be influenced. In addition, the assembly of heteromultimeric isoforms may underlie a structural but temporary change over a circadian period. This study contributes to our understanding of the circadian secretion processes of the pancreatic islet. ERG channels seem to act as part of a system of clock-driven factors, regulating islet-specific secretion processes, possibly in concert with feeding-associated regulators.

Acknowledgements. The skillful assistance of Candy Rothgänger is gratefully appreciated. We also thank Prof. C. Wollheim from the Department of Medicine, University Geneva, Switzerland, for making the INS-1 cell line available to us. The ERG1b-specific antibody was a gift from Dr. G. Robertson (University of Wisconsin-Madison, Madison, WI, USA).

1 Peschke, E. and Peschke, D. (1998) Evidence for a circadian rhythm of insulin release from perifused rat pancreatic islets. Diabetologia 41, 1085 – 1092.
2 Picinato, M. C., Haber, E. P., Carpinelli, A. R. and Cipolla-Neto, J. (2002) Daily rhythm of glucose-induced insulin secretion by isolated islets from intact and pinealectomized rat. J. Pineal Res. 33, 172 – 177.
3 Mühlbauer, E., Wolgast, S., Finckh, U., Peschke, D. and Peschke, E. (2004) Indication of circadian oscillations in the rat pancreas. FEBS Lett. 564, 91 – 96.
4 Balsalobre, A., Damiola, F. and Schibler, U. (1998) A serum shock induces circadian gene expression in mammalian tissue culture cells. Cell 93, 929 – 937.
5 Allaman-Pillet, N., Roduit, R., Oberson, A., Abdelli, S., Ruiz, J., Beckmann, J. S., Schorderet, D. F. and Bonny, C. (2004) Circadian regulation of islet genes involved in insulin production and secretion. Mol. Cell. Endocrinol. 226, 59 – 66.
6 Schuit, F. C., Huypens, P., Heimberg, H. and Pipeleers, D. G. (2001) Glucose sensing in pancreatic beta-cells: a model for the study of other glucose-regulated cells in gut, pancreas, and hypothalamus. Diabetes 50, 1 – 11.
7 Barg, S. (2003) Mechanisms of exocytosis in insulin-secreting B-cells and glucagon-secreting A-cells. Pharmacol. Toxicol. 92, 3 – 13.
8 Su, J., Yu, H., Lenka, N., Hescheler, J. and Ullrich, S. (2001) The expression and regulation of depolarization-activated K^+ channels in the insulin-secreting cell line INS-1. Pflugers Arch. 442, 49 – 56.
9 Yan, L., Figueroa, D. J., Austin, C. P., Liu, Y., Bugianesi, R. M., Slaughter, R. S., Kaczorowski, G. J. and Kohler, M. G. (2004) Expression of voltage-gated potassium channels in human and rhesus pancreatic islets. Diabetes 53, 597 – 607.
10 Itri, J. N., Michel, S., Vansteensel, M. J., Meijer, J. H. and Colwell, C. S. (2005) Fast delayed rectifier potassium current is required for circadian neural activity. Nat. Neurosci. 8, 650 – 656.
11 Yamashita, T., Sekiguchi, A., Iwasaki, Y. K., Sagara, K., Iinuma, H., Hatano, S, Fu, L. T. and Watanabe, H. (2003) Circadian variation of cardiac K^+ channel gene expression. Circulation 107, 1917 – 1922.
12 Panda, S., Antoch, M. P., Miller, B. H., Su, A. I., Schook, A. B., Straume, M., Schultz, P. G., Kay, S. A., Takahashi, J. S. and Hogenesch, J. B. (2002) Coordinated transcription of key pathways in the mouse by the circadian clock. Cell 109, 307 – 320.
13 Storch, K. F., Lipan, O., Leykin, I., Viswanathan, N., Davis, F. C., Wong, W. H. and Weitz, C. J. (2002) Extensive and divergent circadian gene expression in liver and heart. Nature 417, 78 – 83.
14 Rosati, B., Marchetti, P., Crociani, O., Lecchi, M., Lupi, R., Arcangeli, A., Olivotto, M. and Wanke, E. (2000) Glucose- and arginine-induced insulin secretion by human pancreatic beta-cells: the role of HERG K(+) channels in firing and release. FASEB J. 14, 2601 – 2610.
15 Guasti, L., Cilia, E., Crociani, O., Hofmann, G., Polvani, S., Becchetti, A., Wanke, E., Tempia, F and Arcangeli, A. (2005) Expression pattern of the ether-a-go-go-related (ERG) family proteins in the adult mouse central nervous system: evidence for coassembly of different subunits. J. Comp. Neurol. 491, 157 – 174.
16 Schwarz, J. R. and Bauer, C. K. (2004) Functions of erg K^+ channels in excitable cells. J. Cell. Mol. Med. 8, 22 – 30.
17 Jones, E. M., Roti Roti, E. C., Wang, J., Delfosse, S. A. and Robertson, G. A. (2004) Cardiac IKr channels minimally comprise hERG 1a and 1b subunits. J. Biol. Chem. 279, 44690 – 44694.
18 Crociani, O., Guasti, L., Balzi, M., Becchetti, A., Wanke, E., Olivotto, M., Wymore, R. S. and Arcangeli, A. (2003) Cell

cycle-dependent expression of HERG1 and HERG1B isoforms in tumor cells. J. Biol. Chem. 278, 2947 – 2955.
19 Matsuo, T., Yamaguchi, S., Mitsui, S., Emi, A., Shimoda, F. and Okamura, H. (2003) Control mechanism of the circadian clock for timing of cell division *in vivo.* Science 302, 255 – 259.
20 Peschke, E., Muhlbauer, E., Musshoff, U., Csernus, V. J., Chankiewitz, E. and Peschke, D. (2002) Receptor MT(1) mediated influence of melatonin on cAMP concentration and insulin secretion of rat insulinoma cells INS1. J. Pineal Res. 33, 63 – 71.
21 Grundschober, C., Delaunay, F., Puhlhofer, A., Triqueneaux, G., Laudet, V., Bartfai, T. and Nef, P. (2001) Circadian regulation of diverse gene products revealed by mRNA expression profiling of synchronized fibroblasts. J. Biol. Chem. 276, 46751 – 46758.
22 Pfaffl, M. W., Horgan, G. W. and Dempfle, L. (2002) Relative expression software tool (REST) for group-wise comparison and statistical analysis of relative expression results in real-time PCR. Nucleic Acids Res. 30, 1 – 10.
23 Damiola, F., Le Minh, N., Preitner, N., Kornmann, B., Fleury-Olela, F. and Schibler, U. (2000) Restricted feeding uncouples circadian oscillators in peripheral tissues from the central pacemaker in the suprachiasmatic nucleus. Genes Dev. 14, 2950 – 2961.
24 Bazwinsky, I., Bidmon, H. J., Zilles, K. and Hilbig, H. (2005) Characterization of the rhesus monkey superior olivary complex by calcium binding proteins and synaptophysin. J. Anat. 207, 745 – 761.
25 Bach, A. G., Wolgast, S., Muhlbauer, E. and Peschke, E. (2005) Melatonin stimulates inositol-1,4,5-trisphosphate and Ca^{2+} release from INS1 insulinoma cells. J. Pineal Res. 39, 316 – 323.
26 Lipp, P. and Niggli, E. (1993) Ratiometric confocal Ca(2+)-measurements with visible wavelength indicators in isolated cardiac myocytes. Cell. Calcium 14, 359 – 372.
27 Maechler, P. and Wollheim, C. B. (1999) Mitochondrial glutamate acts as a messenger in glucose-induced insulin exocytosis. Nature 402, 685 – 689.
28 Shi, W., Wymore, R. S., Wang, H. S., Pan, Z., Cohen, I. S., McKinnon, D. and Dixon, J. E. (1997) Identification of two nervous system-specific members of the erg potassium channel gene family. J. Neurosci. 17, 9423 – 9432.
29 Korolkova, Y. V., Kozlov, S. A., Lipkin, A. V., Pluzhnikov, K. A., Hadley, J. K., Filippov, A. K., Brown, D. A., Angelo, K., Strobaek, D., Jespersen, T., Olesen, S. P., Jensen, B. S. and Grishin, E. V. (2001) An ERG channel inhibitor from the scorpion *Buthus eupeus.* J. Biol. Chem. 276, 9868 – 9876.
30 Sander, M. and German, M. S. (1997) The beta cell transcription factors and development of the pancreas. J. Mol. Med. 75, 327 – 340.
31 Ueda, H. R., Hayashi, S., Chen, W., Sano, M., Machida, M., Shigeyoshi, Y., Iino, M. and Hashimoto, S. (2005) System-level identification of transcriptional circuits underlying mammalian circadian clocks. Nat. Genet. 37, 187 – 192.
32 Asfari, M., Janjic, D., Meda, P., Li, G., Halban, P. A. and Wollheim, C. B. (1992) Establishment of 2-mercaptoethanol-dependent differentiated insulin-secreting cell lines. Endocrinology 130, 167 – 178.
33 Lees-Miller, J. P., Guo, J., Somers, J. R., Roach, D. E., Sheldon, R. S., Rancourt, D. E. and Duff, H. J. (2003) Selective knockout of mouse ERG1 B potassium channel eliminates I(Kr) in adult ventricular myocytes and elicits episodes of abrupt sinus bradycardia. Mol. Cell. Biol. 23, 1856 – 1862.
34 Wimmers, S., Bauer, C. K. and Schwarz, J. R. (2002) Biophysical properties of heteromultimeric erg K+ channels. Pflugers Arch. 445, 423 – 430.
35 Hirdes, W., Schweizer, M., Schuricht, K. S., Guddat, S. S., Wulfsen, I., Bauer C. K. and Schwarz J. R. (2005) Fast erg K^+ currents in rat embryonic serotonergic neurones. J. Physiol. 564, 33 – 49.
36 Overholt, J. L., Ficker, E., Yang, T., Shams, H., Bright, G. R. and Prabhakar, N. R. (2000) HERG-like potassium current regulates the resting membrane potential in glomus cells of the rabbit carotid body. J. Neurophysiol. 83, 1150 – 1157.